Unoccupied electronic states of icosahedral Al-Pd-Mn quasicrystals: Evidence of image potential resonance and pseudogap

M. Maniraj, Abhishek Rai, S. R. Barman, M. Krajčí, D. L. Schlagel, T. A. Lograsso, and K. Horn

Phys. Rev. B **90**, 115407 — Published 5 September 2014

DOI: 10.1103/PhysRevB.90.115407

Unoccupied electronic states of icosahedral Al-Pd-Mn quasicrystal: evidence of image potential resonance and pseudogap

M. Maniraj, Abhishek Rai, and S. R. Barman*
UGC-DAE Consortium for Scientific Research, Khandwa Road, Indore, 452001, Madhya Pradesh, India

M. Krajčí
Institute of Physics, Slovak Academy of Sciences, Dúbravská cesta 9, SK-84511 Bratislava, Slovak Republic

D. L. Schlagel and T. A. Lograsso
Division of Materials Sciences and Engineering, Ames Laboratory, Ames Iowa 500011-3020, USA

K. Horn
Fritz-Haber-Institut der Max-Planck-Gesellschaft, 14195 Berlin, Germany

We study the unoccupied region of the electronic structure of the fivefold symmetric surface of an icosahedral (i) Al-Pd-Mn quasicrystal. A feature that exhibits parabolic dispersion with an effective mass of (1.15±0.1)m_e and tracks the change in the work function is assigned to an image potential resonance because our density functional calculation shows absence of band gap in the respective energy region. We show that Sn grows pseudomorphically on i-Al-Pd-Mn as predicted by density functional theory calculations and the energy of the image potential resonance tracks the change in the work function with Sn coverage. The image potential resonance appears much weaker in the spectrum from the related crystalline Al-Pd-Mn surface, demonstrating that its strength is related to the compatibility of the quasiperiodic wave functions in i-Al-Pd-Mn with the free electron like image potential states. Our investigation of the energy region immediately above E_F provides unambiguous evidence for the presence of a pseudogap, in agreement with our density functional theory calculations.

I. INTRODUCTION

Quasicrystals are an intriguing class of materials since they defy the familiar concept that relates atomic order in solids with translational symmetry. In spite of 30 years of intense research, the origin of aperiodic quasicrystalline ordering is far from fully understood. The formation of a pseudogap near the Fermi level (E_F) has been related to a Fermi surface-quasi Brillouin zone interaction mechanism.[1,2] An increasing body of evidence has supported this notion[3,4] indicating the presence of a pseudogap in the bulk, while the surface may behave differently.[5,6] The bulk electronic structure of quasicrystals recently studied by hard x-ray photoelectron spectroscopy demonstrates presence of a pseudogap.[6] On the other hand, low energy photoemission studies that are surface sensitive, did not reveal a clear signature of the pseudogap. Angle resolved photoemission on icosahedral(i) Al-Pd-Mn,[7] show a weak quasiperiodic dispersion of electronic band at about 2.5 eV below the E_F, while a free-electron-like band dispersion has been reported for decagonal Al-Ni-Co.[8] Here, we extend wavevector resolved studies of the electronic structure of quasicrystalline surfaces to the region of the unoccupied states. We concentrate on three features: the region of the pseudogap immediately near E_F, the overall density of state (DOS) peaks, and a strongly dispersive feature near the vacuum level. Through density functional theory (DFT) based calculations for Al-Pd-Mn, we are able to interpret all spectral features in a consistent picture. Our interpretation is also based on a direct comparison of spectral features from the icosahedral (000001) surface and its crystalline $Al_{65}Pd_{31}Mn_4$ counterpart of cubic symmetry, and changes induced by depositing Sn on the surface in order to vary the work function of the aperiodic surface.

II. EXPERIMENTAL AND CALCULATION DETAILS

The momentum resolved inverse photoemission spectroscopy (IPES) experiments were performed in a multilevel chamber at a base pressure of 5×10^{-11} mbar. The measurements were carried out using a CaF_2/acetone bandpass photon detector[9,10] with a Stoffel-Johnson design electron source.[11,12] The total energy resolution was about 0.5 eV, while the momentum resolution is about 0.13 $Å^{-1}$. The electron beam current variation as a function of kinetic energy was accounted for by normalizing the measured counts by the sample current at each step, as in our previous studies.[13] IPES was performed by varying the polar angle of the specimen, while the electron source and the detector were kept fixed at an angle of 45°. A single grain i-$Al_{69.4}Pd_{20.8}Mn_{9.8}$ quasicrystal cut perpendicular to its five-fold axis was cleaned in vacuum by repeated cycles of Ar^+ ion sputtering with 1.5 keV for 1 h and followed by annealing up to 930 K for 2−2.5 h[14] in a specially designed sample holder.[15] A relatively Pd-rich,

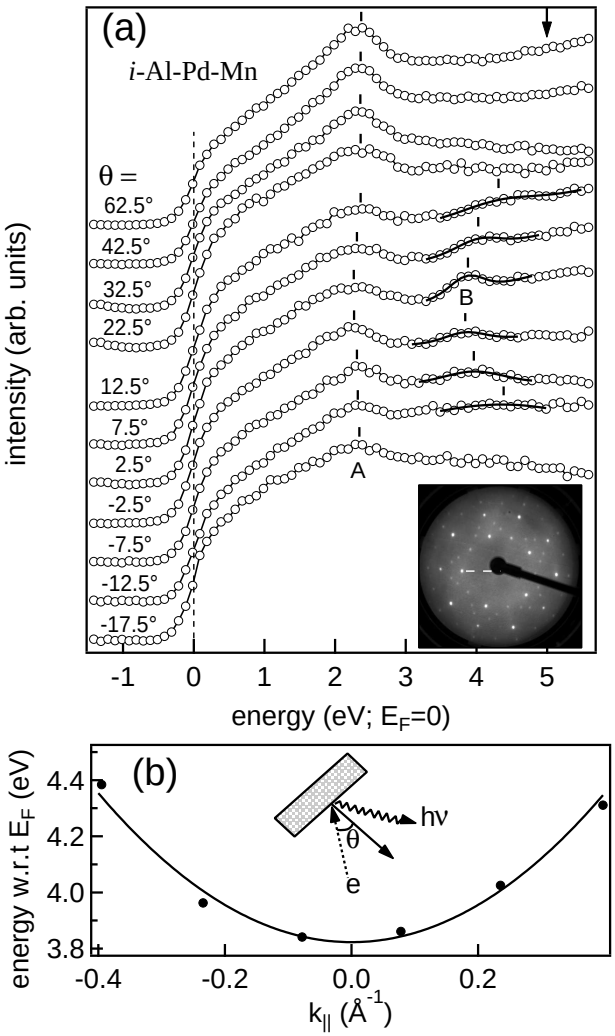

FIG. 1: (a) The IPES spectra measured as a function of the electron incident angle θ for the five-fold surface of i-Al-Pd-Mn. The arrow indicates E_{vac}. Least square curve fitting was performed to simulate feature B by a Guassian function (continuous lines). The inset shows the LEED pattern recorded with E_p= 81 eV. The dashed line indicates the direction of IPES measurement for the positive θ. (b) The dispersion of feature B with $k_{\|}$ is fitted by a parabola (solid line). The experimental geometry is shown as an inset.

crystalline (cubic symmetry) c-Al-Pd-Mn surface with a composition of $Al_{65}Pd_{31}Mn_4$ was prepared by annealing around 650 K for 3 h.[16] Sn was deposited on i-Al-Pd-Mn at room temperature using a water cooled Knudsen cell.[17] The Sn adlayer coverage was calculated from the area under the Sn 3d and Al 2p core-levels.[17,18]

The *ab initio* DFT calculations of the electronic structure were performed using the VASP code.[19,20] The structural model of bulk i-Al-Pd-Mn was constructed using the cut-and-projection technique in the six-dimensional hyperspace according to the Katz-Gratias-Boudard model.[21,22] The i-Al-Pd-Mn quasicrystal is represented by a 2/1 approximant consisting of 544 atoms in a cubic cell (396 Al atoms, 100 Pd atoms, 48 Mn atoms) with the lattice constant $a = 20.31$ Å and the $P2_13$ space-group symmetry (No. 198). An approximant has a local structure that is very similar to quasicrystals, but is periodic with very large unit cells. The approximants are obtained by choosing the Fibonacci ratio n_L/n_S, where n_L and n_S are the numbers of long (L) and short (S) tiles the Fibonacci sequence.

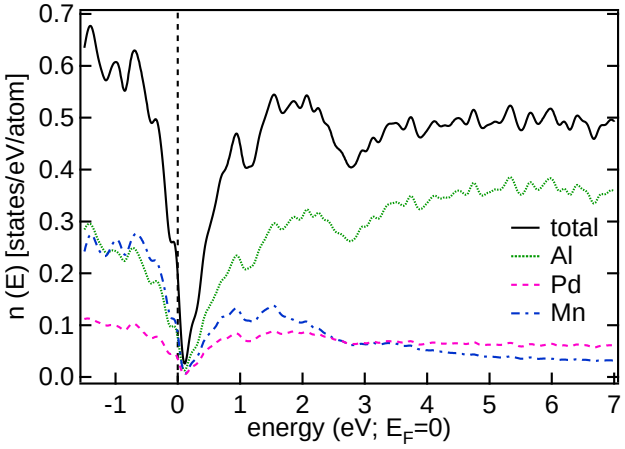

FIG. 2: Total and Al, Pd and Mn partial density of states of Al-Pd-Mn calculated by density functional theory using the VASP code.

III. RESULTS AND DISCUSSION

The IPES spectra of i-Al-Pd-Mn in Fig. 1(a) show two well-defined features, marked by A and B. Feature A, which is observed around 2.3 eV, exhibits a small dispersion of about 100 meV within the entire incidence angle (θ) range. We attribute this feature primarily to Al s,p-Mn 3d hybridized states, by comparison of the spectra with the broad feature centered around 2 eV in the calculated DOS in Fig. 2 that displays the total and Al, Pd, and Mn partial DOS. Feature B, in contrast to feature A, displays a considerable dispersion from 3.8 to 4.4 eV above E_F. We have performed least square curve fitting using a Gaussian function to determine its energy position (solid lines in Fig. 1(a)). A plot of the energy versus momentum parallel to the surface ($k_{\|}$) shows a parabolic dispersion with an effective mass of m^*= (1.15±0.1)m_e, where m_e is the free electron mass (Fig. 1(b)). Since no such feature is present in the DOS in this energy range, feature B cannot be assigned to a feature related to the electronic states of a quasicrystal.

Dispersing electron states below E_F in quasicrystalline materials have been observed in angle resolved photoemission,[7,8] and may in principle also be present in the unoccupied region. However, the experimental data shown here strongly suggest that feature B is not related

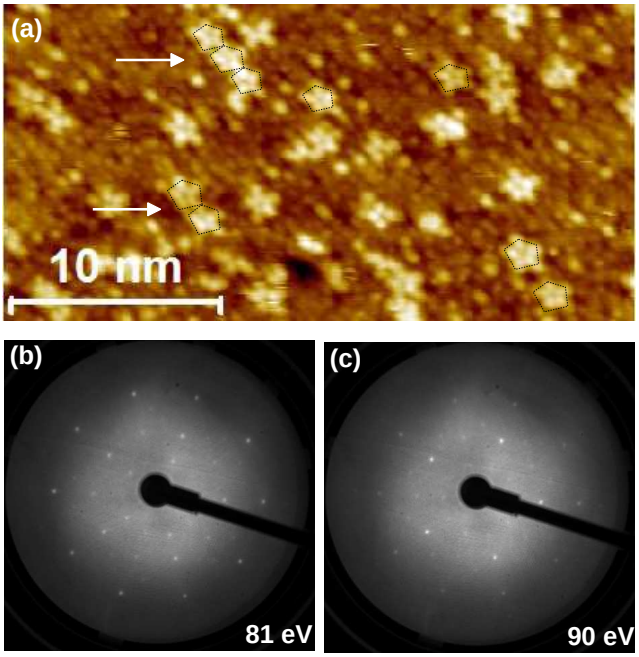

FIG. 3: (a) Constant current (I_T= 1.1 nA, U_T= 0.8 V) STM topography image of Sn pentagonal stars (white arrow) on *i*-Al-Pd-Mn. Low energy electron diffraction patterns of 1 ML Sn/*i*-Al-Pd-Mn recorded with electron energy of (b) 81 eV and (c) 90 eV.

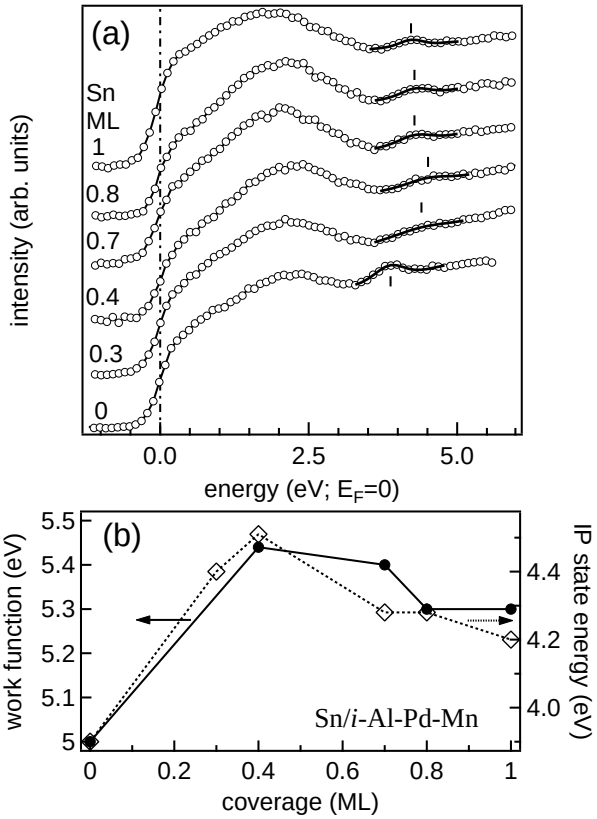

FIG. 4: (a) The IPES spectra of Sn/*i*-Al-Pd-Mn measured at room temperature in normal incidence geometry. The black continuous lines are the fitted curves obtained using a Gaussian function. (b) The work function (continuous line) and the energy of the image potential resonance (dotted line) as a function of Sn coverage.

to the bulk electronic structure of *i*-Al-Pd-Mn, but rather an image potential-related feature that can exist in the potential well created by the interaction of the electron with its image in the metal surface.[23] Since the image potential is related to the vacuum level, an image potential state/resonance will exhibit an energy shift upon a change in work function. This is a standard method to identify an image potential state in IPES, and to distinguish it from other kinds of surface or bulk-related states.[24] Here, we use the work function change induced by Sn adsorption. This material forms a well- ordered pseudomorphic layer, thus avoiding scattering processes that might suppress the image potential state. Pseudomorphic growth of single layers of Sn on *i*-Al-Pd-Mn had been predicted in an earlier theoretical work,[25] and we provide direct experimental proof for this through scanning tunneling microscopy (STM) and low energy electron diffraction (LEED) in Fig. 3. The pentagonal star-shaped features (Fig. 3(a)), which are similar to those found for Bi, Sb[26] and Pb,[27,28] nucleate at the bright 'flowers' of the *i*-Al-Pd-Mn surface and have a dimension of 0.6±0.1 nm (a side of the pentagon). These pentagonal stars merge to form a uniform layer at higher coverage, as demonstrated by the sharp five-fold low energy electron diffraction patterns (LEED) in Fig. 3(b-c); a detailed study of this system is presented elsewhere.[29]

In the normal incidence IPES spectra of Sn/i-Al-Pd-Mn (Fig. 4(a)), feature B is shown as a function of Sn coverage; its energy changes with the work function induced by an increasing coverage as shown in Fig. 4(b), measured from the secondary edge cutoff of the ultraviolet photoemission spectra. The work function change with Sn adsorption is largest for 0.4 monolayer (ML), where it increases to 5.45±0.15 eV, before dropping again an monolayer completion to 5.3±0.15 eV. The direct comparison of the work function change and the shift of peak B with coverage (Fig. 4(b)) shows a close correspondence. This shows that feature B is indeed related to the image potential, and its shift due to Sn deposition is caused by the change in work function. Image potential states are Rydberg series of bound states whose binding energy is given by $E_n = 0.85/n^2$ eV, where n= 1, 2, 3,... and have been reported in many metal surfaces.[23,24,30–33] They are pinned to the vacuum level (E_{vac}) and thus the energy of n= 1 image potential state is 0.85 eV below E_{vac}.

The work function of *i*-Al-Pd-Mn turns out to be 5± 0.15 eV, and the resulting E_{vac} is shown by an arrow in Fig. 1(a). A slightly smaller value of the work function (4.75− 4.91 eV) was reported previously from low-energy electron microscopy.[34] Considering the uncertainty of measurement of the work function ranging from

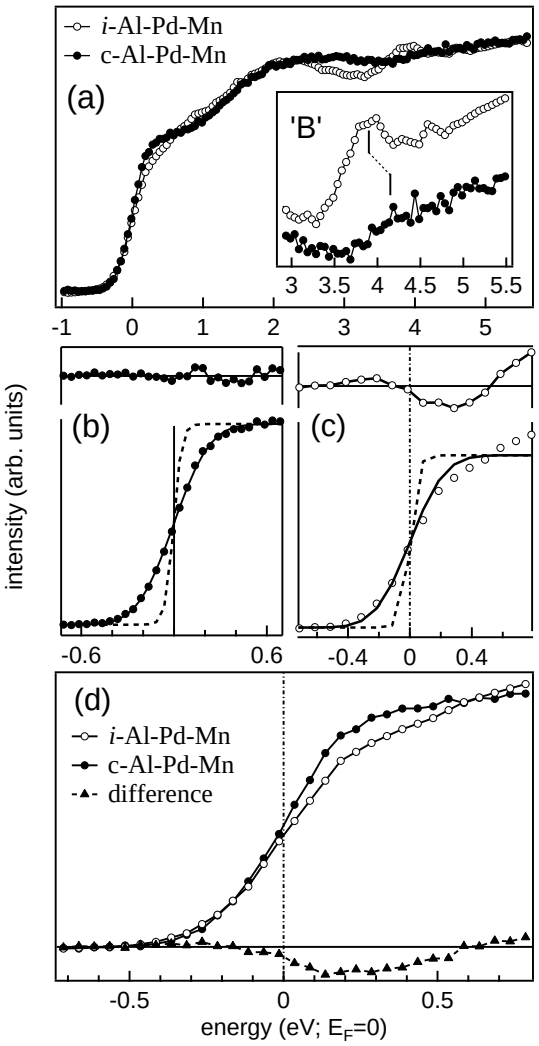

FIG. 5: (a) Comparison of the near normal incidence inverse photoemission spectra measured for bare *i*-Al-Pd-Mn quasicrystal (open circle) and *c*-Al-Pd-Mn (filled circle) surface. The inset shows the closeup of the image potential resonance region. The Fermi edge region of (b) *c*-Al-Pd-Mn (filled circle) and (c) *i*-Al-Pd-Mn (open circle) along with the least square fitted curve (solid line) and the Fermi-Dirac distribution function (dashed line). The residual of the fitting is shown at the top. (d) The Fermi edge region of the spectra in (a) shown in an expanded scale along with the difference spectrum (filled triangles).

4.75 to 5 eV, the position of feature B (0.85-1.1 eV below E_{vac} for normal incidence) is close to the expected value (0.85 eV) for the n= 1 image potential state. While the width of an image potential state is very small (16 meV for n= 1),[35,36] the experimental energy resolution is much larger (0.5 eV). Thus, the width of this state is governed by the experimental resolution only and from the least square curve fitting (solid lines in Fig. 4(a)), we find that the width (0.5±0.05 eV) for both bare and Sn covered Al-Pd-Mn agrees with this quantity.

Although the above-mentioned characteristics of feature B are strongly indicative of an image potential state, it is puzzling to note that the DOS in Fig. 2 does not show the presence of any gap in this energy region. This raises the question about the origin of the barrier that confines the image potential states. Generally, for crystalline surfaces, such features observed in the absence of a gap are referred to as image potential resonance. The band dispersion calculated for Al-Pd-Mn along the high symmetry axes such as two-, three-, and five-fold do not show evidence of any gap in this energy region.[21] This indicates that the state giving rise to feature B is actually an image potential resonance, where the potential step at the vacuum-substrate interface provides a large enough barrier for such states to exist.

Examining the image potential resonance for icosahedral and cubic *i.e.* periodic surfaces of Al-Pd-Mn provides an interesting comparison to investigate a possible influence of quasiperiodic ordering on the nature of the potential barrier at the surface. An image potential feature is also observed for crystalline (*c*-) *c*-Al-Pd-Mn, but its position is shifted to higher energy due to an increased work function (5.2 eV) of *c*-Al-Pd-Mn by 0.2 eV compared to that of *i*-Al-Pd-Mn (5 eV) (as shown in Fig. 5(a) and its inset). Its intensity in case of *c*-Al-Pd-Mn is strongly suppressed compared to *i*-Al-Pd-Mn. We assign this effect to a stronger coupling with, and decay into, the periodic bulk states in the crystalline surface. The larger intensity of the image potential feature (*i.e.* feature B) on the quasicrystalline surface is thus due to a stronger reflection of the free electron like wave function of the image potential states by the *i*-Al-Pd-Mn substrate with its quasiperiodic symmetry of the wave functions.

Turning to the question of the existence of pseudogap in the unoccupied states, which is of central importance for an understanding of quasicrystal formation, consider the IPES spectra of *c*- and *i*-Al-Pd-Mn in the vicinity of E_F (Fig. 5). We fit the respective data by a Fermi-Dirac distribution convoluted with a Gaussian to account for the instrumental broadening to simulate the experimental spectrum. A good fit is obtained for *c*-Al-Pd-Mn (see the residual on top of Fig. 5(b)), showing that this surface has a metallic character. However, the fit for *i*-Al-Pd-Mn, where the E_F position and the energy resolution obtained from *c*-Al-Pd-Mn are kept unchanged, exhibiting large deviations (Fig. 5(c)) from the Fermi-Dirac distribution showing that the spectral function has a different shape. This is clearly evident from the comparison of the two spectra in Fig. 5(d). The lower intensity from E_F onwards in *i*-Al-Pd-Mn gives evidence for the existence of a pseudogap in this material. This observation is supported by the calculated DOS in Fig. 2 that shows the existence of a pseudogap with a minimum slightly above E_F. However, since IPES is a surface sensitive technique, the pseudogap observed here is weaker compared to the bulk, as shown by our recent hard x-ray photoemission spectroscopy study.[6]

IV. CONCLUSION

In summary, our study of the unoccupied electron states of *i*-Al-Pd-Mn using inverse photoemission spectroscopy establishes the existence of the pseudogap and an image potential resonance. Two features are observed in the IPES spectra, a nondispersive one, and one that exhibits parabolic dispersion with an effective mass of $(1.15\pm0.1)m_e$. Based on our density functional theory (DFT) calculations, we assign the former to Al *s*, *p*- Mn 3*d* hybridized density of states peak. The dispersing state is identified as an image potential resonance based on our DFT calculation that shows absence of any band gap. It tracks the change in work function of *i*-Al-Pd-Mn surface as a function of Sn coverage. The differences of the image potential resonance between the crystalline and quasicrystalline Al-Pd-Mn surface are ascribed to the quasiperiodic symmetry of the substrate wave functions, which are incompatible with that of the image potential resonance. Pseudogap is unambiguously identified above E_F, in excellent agreement with our theoretical calculation.

V. ACKNOWLEDGMENT

We thank A. K. Shukla, S. Singh, S. W. D′Souza, J. Nayak, and N. Ghodke for useful discussions and support. This work has been supported by the Max Planck partner group project. M.M. is grateful to the Council of Scientific and Industrial Research, New Delhi for research fellowship. M.K. is thankful to Slovak Grant Agency VEGA (No. 2/0111/11). TAL and DL acknowledge the support of the U.S. Department of Energy (DOE), Office of Science, Basic Energy Sciences, Materials Science and Engineering Division.

*Electronic mail: barmansr@gmail.com

[1] W. Hume-Rothery, J. Inst. Met. **35**, 295 (1926); H. Jones, Proc. Phys. Soc. London **49**, 250 (1937).
[2] J. Hafner and M. Krajčí, Phys. Rev. Lett. **68**, 2321 (1992).
[3] Z. M. Stadnik *et al.*, Phys. Rev. Lett. **77**, 1777 (1996); Phys. Rev. B **55**, 10938 (1997); Phys. Rev. B **64**, 214202 (2001).
[4] D. N. Davydov, D. Mayou, C. Berger, C. Gignoux, A. Neumann, A. G. M. Jansen, and P. Wyder, Phys. Rev. Lett. **77**, 3173 (1996).
[5] G. Neuhold, S. R. Barman, K. Horn, W. Theis, P. Ebert, and K. Urban, Phys. Rev. B **58**, 734 (1998).
[6] J. Nayak, M. Maniraj, A. Rai, S. Singh, P. Rajput, A. Gloskovskii, J. Zegenhagen, D. L. Schlagel, T. A. Lograsso, K. Horn, and S. R. Barman, Phys. Rev. Lett. **109**, 216403 (2012).
[7] X. Wu, S . W. Kycia, C. G. Olson, P. J. Benning, A. I. Goldman, and D. W. Lynch, Phys. Rev. Lett. **75**, 4540 (1995).
[8] E. Rotenberg, W. Theis, K. Horn and P. Gille, Nature **406**, 602 (2000).
[9] S. Banik, A. K. Shukla, and S. R. Barman, Rev. Sci. Instrum. **76**, 066102 (2005); A. K. Shukla, S. Banik, and S. R. Barman, Curr. Sci. **90**, 490 (2006).
[10] M. Maniraj, S. W. D'Souza, J. Nayak, A. Rai, S. Singh, B. N. Raja Sekhar, and S. R. Barman, Rev. Sci. Instrum. **82**, 093901 (2011); Rev. Sci. Instrum. **83**, 046107 (2012).
[11] N. G. Stoffel and P. D. Johnson, Phys. Res. A, **234**, 230 (1985).
[12] M. Maniraj and S. R. Barman, Rev. Sci. Instrum. **85**, 033301 (2014).
[13] R. Kundu, P. Mishra, B. R. Sekhar, M. Maniraj, and S. R. Barman, Physica B **407**, 827 (2012); S. K. Pandey, A. Kumar, S. Banik, A. K. Shukla, S. R. Barman, and A. V. Pimpale, Phys. Rev. B **77**, 113104 (2008); R. S. Dhaka *et al.*, Phys. Rev. B **78**, 073107 (2008).
[14] A. K. Shukla, R. S. Dhaka, S. W. D'Souza, Sanjay Singh, D. Wu, T. A. Lograsso, M. Krajčí, J. Hafner, K. Horn, and S. R. Barman, Phys. Rev. B **79**, 134206 (2009).
[15] R. S. Dhaka, A. K. Shukla, M. Maniraj, S. W. D'Souza, J. Nayak, and S. R. Barman, Rev. Sci. Instrum. **81**, 043907 (2010).
[16] Z. Shen, M. J. Kramer, C. J. Jenks, A. I. Goldman, T. Lograsso, D. Delaney, M. Heinzig, W. Raberg, and P. A. Thiel, Phys. Rev. B **58**, 9961 (1998).
[17] A. K. Shukla, S. Banik, R. S. Dhaka, C. Biswas, S. R. Barman and H. Haak, Rev. Sci. Instrum. **75**, 4467 (2004).
[18] A. K. Shukla, R. S. Dhaka, S. W. D'Souza, M. Maniraj, S. R. Barman, K. Horn, Ph. Ebert, K. Urban, D. Wu and T. A. Lograsso, J. Phys.: Condens. Matter **21**, 405005 (2009).
[19] G. Kresse and J. Furthmüller, Phys. Rev. B **54**, 11169 (1996).
[20] G. Kresse and D. Joubert, Phys. Rev. B **59**, 1758 (1999).
[21] M. Krajčí M. Windisch, J. Hafner, G. Kresse, and M. Mihalkovič, Phys. Rev. B **51**, 17355 (1995).
[22] M. Krajčí and J. Hafner, Phys. Rev. B **84**, 214419 (2009).
[23] P. M. Echenique and J. B. Pendry, J. Phys. C **11**, 2065 (1978).
[24] V. Dose, W. Altmann, A. Goldmann , U. Kolac and J. Rogozik, Phys. Rev. Lett. **52**, 1919 (1984); V. Dose, Phys. Scr. **36**, 669 (1987).
[25] M. Krajčí, and J. Hafner, Phys. Rev. B **71**, 184207 (2005).
[26] K. J. Franke, H. R. Sharma, W. Theis, P. Gille, Ph. Ebert, and K. H. Rieder, Phys. Rev. Lett. **89** 156104 (2002).
[27] J. Ledieu, L. Leung, L. H. Wearing, R. McGrath, T. A. Lograsso, D. Wu, and V. Fournée, Phys. Rev. B **77**, 073409 (2008).
[28] J. Ledieu, M. Krajčí, J. Hafner, L. Leung, L. H. Wearing, R. McGrath, T. A. Lograsso, D. Wu, and V. Fournée, Phys. Rev. B **79**, 165430 (2009).
[29] M. Maniraj *et al.* (to be published).
[30] R. M. Osgood and X. Wang, Solid State Phys. **51**, 1 (1998).
[31] D. Straub and F. J. Himpsel, Phys. Rev. Lett. **52**, 1922 (1984); Phys. Rev. B **33**, 2256 (1986).

[32] S. Yang, R. A. Bartynski, G. P. Kochanski, S. Papadia, T. Fondén, M. Persson, Phys. Rev. Lett. **70**, 849 (1993).
[33] C. Eibl, A. B. Schmidt, and M. Donath, Phys. Rev. B **86**, 161414(R) (2012).
[34] B. Ünal, Y. Sato, K. F. McCarty, N. C. Bartelt, T. Duden, C. J. Jenks, A. K. Schmid, and P. A. Thiel, J. Vac. Sci. Technol. A **27**, 1249 (2009).
[35] U. Höfer, I. L. Shumay, Ch. Reuß, U. Thomann, W. Wallauer, and Th. Fauster, Science **277**, 1480 (1997).
[36] S. Schuppler, N. Fischer, Th. Fauster, and W. Steinmann, Phys. Rev. B **46**, 13539 (1992).